International Journal of Thermophysics, Vol. 16, No. 2, 1995

Vapor–Liquid Equilibria of Ternary Mixtures in the Critical Region on Paths of Constant Temperature and Overall Composition[1]

L. J. Van Poolen[2] and J. C. Rainwater[3,4]

High-pressure vapor–liquid equilibrium (VLE) data for the ternary mixture ethane + *n*-butane + *n*-pentane due to Thodos and co-workers have been correlated by a ternary version of the modified Leung–Griffiths model. Data were taken along paths of constant temperature and approximately constant overall composition, and a separate test was made for such constancy. Seventeen different specified overall compositions at four different temperatures were correlated. In general, agreement between the correlation and data is very good, particularly for those curves that satisfy the test for constant overall composition. The ternary model has been constructed from correlations of each of the three constituent binaries without any further adjustable parameters.

KEY WORDS: critical region; ethane; Leung–Griffiths model; *n*-butane; *n*-pentane; phase rule; ternary mixtures; vapor–liquid equilibrium.

1. INTRODUCTION

The Leung–Griffiths model [1], as modified by Moldover, Rainwater, and co-workers [2–4], has for many years been applied to critical-region vapor–liquid equilibrium (VLE) of binary mixtures. More recently, Lynch et al. [5] successfully generalized the model to ternary hydrocarbon mixtures, and Jacobsen et al. [6] applied it to air (nitrogen–oxygen–argon). Also, Smith and Lynch [7] extended the model to mixtures of four and five components. Lynch et al. [5] applied the model to data of Thodos and co-workers [8–11] along loci of constant temperature and overall

---

[1] Paper presented at the Twelfth Symposium on Thermophysical Properties, June 19–24, 1994, Boulder, Colorado, U.S.A.

[2] Engineering Department, Calvin College, Grand Rapids, Michigan 49546, U.S.A.

[3] Thermophysics Division, National Institute of Standards and Technology, Boulder, Colorado 80303, U.S.A.

[4] Author to whom correspondence should be addressed.

0195-928X/95/0300-0473$07.50/0 © 1995 Plenum Publishing Corporation

composition, but the constancy of overall composition was not considered as a constraint in that analysis.

In this work we apply a ternary version of the modified Leung–Griffiths model to the data of Thodos and co-workers on the system ethane + *n*-butane + *n*-pentane, with attention to the (intended) constancy of overall composition in the experimental data. The model differs in some respects from that of Lynch et al., but has the common feature that the ternary thermodynamic surface is constructed from correlations of the three constituent binary systems without any further parameters.

2. THE THERMODYNAMIC PATH

Figure 1 shows the experimental thermodynamic path that has been followed by Thodos and co-workers for a number of ternary [8–11]

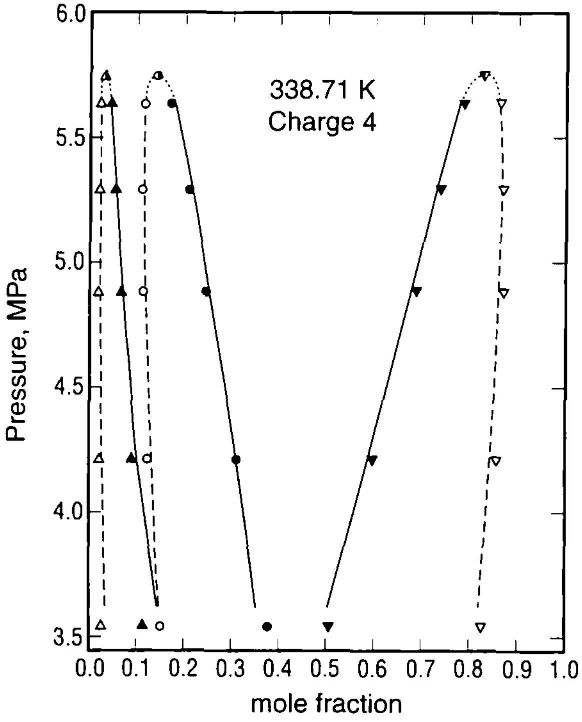

Fig. 1. Critical and coexisting states for charge 4, $T = 338.71$ K. Triangles, *n*-pentane; circles, *n*-butane; inverted triangles, ethane; half-filled symbols, critical point; filled symbols, liquid; open symbols, vapor; solid lines, model bubble curves; dashed lines, dew curves.

systems. A specific "charge," or mixture of specified composition, is prepared and the critical temperature is estimated by an empirical formula [12]. The top of the figure shows the mixture critical point and the composition of the charge in terms of x_1 (*n*-pentane), x_2 (*n*-butane), and x_3 (ethane). It is somewhat redundant in that $x_1 + x_2 + x_3 = 1$ for all experimental and theoretical points, but the complete display is instructive.

At first the mixture is in a supercritical state just above its critical pressure and at its (estimated) critical temperature. The pressure is then lowered so that the system passes into a two-phase region with separate liquid and vapor compositions, as shown. As the pressure is further lowered, the system exits the two-phase region into a one-phase vapor state. Thus in principle, at the bottom of the diagram, the vapor composition returns to that of the overall charge and the critical point composition, while the liquid state at lowest pressure represents the composition of the dew just before complete vaporization.

Since the system is closed, in principle the overall composition should remain constant. According to the generalized phase rule of Van Poolen [13], the constraints of constant temperature and overall composition on a two-phase path result in one degree of freedom, allowing, in this case, pressure variation. In practice, however, the composition changes slightly from sampling or leakage. Although Thodos and co-workers evidently did not apply such a test, the constancy of overall composition can be tested

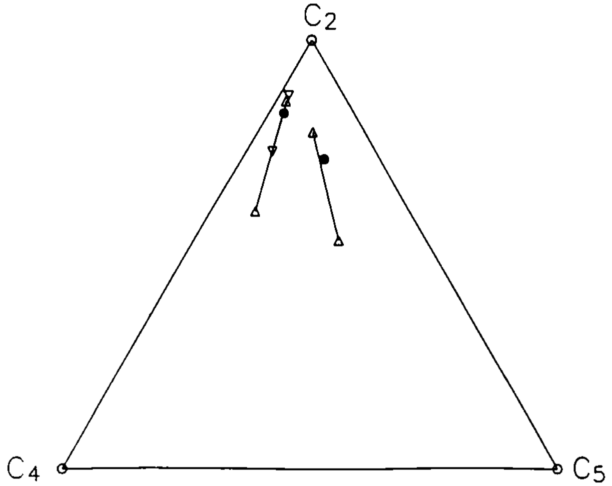

Fig. 2. Triangle diagram showing test for constant overall composition. Filled circles, total composition; open symbols, coexisting liquid and vapor states; left group of symbols, $T = 338.71$ K, charge 4, small R_d; right group, $T = 366.48$ K, charge 3, larger R_d.

easily with a triangle diagram such as Fig. 2. Here the equilateral triangle has unit altitude, and for a point in the triangle, x_i is the perpendicular distance to side jk, $i \neq j \neq k$. From material balance considerations, the straight tie line between coexisting liquid and vapor points should intersect the point of overall charge composition. If it does not, the perpendicular drop distance from the point of overall composition to the tie line is a good measure of deviation from constancy of overall composition.

3. THE TERNARY LEUNG–GRIFFITHS MODEL

We now briefly describe our ternary model and compare it to the somewhat different version of Ref. 5. The two-phase region is characterized by the variable t and any two of the three variables $\zeta_1, \zeta_2, \zeta_3$ where

$$\zeta_i = K_i e^{\mu_i/RT} \Big/ \sum_{i=1}^{3} K_i e^{\mu_i/RT} \tag{1}$$

$$t = [T - T_c(\zeta_i, \zeta_j)]/T_c(\zeta_i, \zeta_j) \tag{2}$$

so that $\zeta_1 + \zeta_2 + \zeta_3 = 1$. Here K_i are constants (or can be temperature dependent [14]), μ_i is the chemical potential of fluid i, R is the gas constant, T is temperature, and the subscript c denotes critical. The critical surface ($t = 0$) is given by the following generic form, where A_c is inverse critical temperature, critical pressure–temperature ratio (P_c/T_c), or critical density ρ_c:

$$\begin{aligned} A_c(\zeta_1, \zeta_2, \zeta_3) = {} & \sum_{i=1}^{3} \zeta_i A_c^{(i)} + \zeta_3\zeta_2 \sum_{k=0}^{3} B_i^{(32)}(1 - 2\zeta_3)^k \\ & + \zeta_2\zeta_1 \sum_{k=0}^{3} B_i^{(21)}(1 - 2\zeta_2)^k + \zeta_3\zeta_1 \sum_{k=0}^{3} B_i^{(31)}(1 - 2\zeta_3)^k \end{aligned} \tag{3}$$

cf. Ref. 5, Eqs. (25)–(27), where on the critical surface the mole fraction of fluid i is given by $x_i = \zeta_i$ [14]. In this work, the parameter H_1 [3] that modifies this relation is not used.

In the two-phase region ($t < 0$), coexisting densities and pressure–temperature ratios are

$$\rho = \rho_c[1 \pm C_1(-t)^{0.355} + C_2 t] \tag{4}$$

$$\frac{P}{RT} = \frac{P_c}{RT_c}[1 + C_3(-t)^{1.9} + C_4 t + C_5 t^2 + C_6 t^3] \tag{5}$$

where plus is for liquid and minus for vapor, and C_k, as well as the critical parameters, depend on (ζ_i, ζ_j). As in Ref. 5 and the binary model, the C_k functions in Eq. (5) are simple linear interpolations of the pure C_k values. However, C_1 and C_2 for binaries involve the parameters C_H, C_X, C_Z, C_Y, and C_R, which depend on the particular mixture [3, 4]. For generalizations to ternaries, we define quantities (note parentheses vs. square brackets),

$$C^{(123)} = \frac{\zeta_1\zeta_2 C^{(12)} + \zeta_1\zeta_3 C^{(13)} + \zeta_2\zeta_3 C^{(23)}}{\zeta_1\zeta_2 + \zeta_1\zeta_3 + \zeta_2\zeta_3} \tag{6}$$

$$C^{[123]} = \frac{\zeta_1^2\zeta_2^2 C^{(12)} + \zeta_1^2\zeta_3^2 C^{(13)} + \zeta_2^2\zeta_3^2 C^{(23)}}{\zeta_1\zeta_2 + \zeta_1\zeta_3 + \zeta_2\zeta_3} \tag{7}$$

For ternary mixtures, C_2 in Eq. (4) generalizes to

$$C_2(\zeta_i, \zeta_j) = \sum_{i=1}^{3} C_2^{(i)}\zeta_i + C_R^{[123]} \tag{8}$$

where $C_2^{(i)}$ is the pure-fluid coefficient. For C_1, we first define the function

$$\bar{Q}_i(\zeta_1, \zeta_2, \zeta_3, t) = \left(\frac{\partial\omega}{\partial\zeta_i}\right)_{t,\zeta_j} + \left(\frac{\partial\omega}{\partial t}\right)_{\zeta_i,\zeta_j} \left(\frac{\partial B_c}{\partial\zeta_i}\right)_{\zeta_j} \frac{1+t}{B_c}; \quad i = 2, 3; \quad j \neq i \tag{9}$$

where $\omega = P/RT$ depends on (ζ_i, ζ_j, t) and $B_c = 1/RT_c$ depends on (ζ_i, ζ_j). Also, we define Q_{i0} to be Q_i evaluated at $t = 0$. For ternary mixtures C_1 is then

$$C_1(\zeta_1, \zeta_2, \zeta_3) = \sum_{i=1}^{3} \zeta_i C_1^{(i)}/(1 + C'_X J) \tag{10}$$

where

$$J = \frac{(\zeta_1\zeta_3 + \zeta_2\zeta_3)[\zeta_3(\zeta_2 + \zeta_1)\,\bar{Q}_{30} - \zeta_3\zeta_2\bar{Q}_{20}]}{(\zeta_1\zeta_2 + \zeta_1\zeta_3 + \zeta_2\zeta_3)\,\rho_c(\zeta_1, \zeta_2, \zeta_3)} + \frac{\zeta_1\zeta_2[(\zeta_1 + \zeta_3)\,\zeta_2\bar{Q}_{20} - \zeta_2\zeta_3\bar{Q}_{30}]}{(\zeta_1\zeta_2 + \zeta_1\zeta_3 + \zeta_2\zeta_3)\,\rho_c(\zeta_1, \zeta_2, \zeta_3)} \tag{11}$$

$$C'_X = C_X^{(123)}(1 + C_Y^{(123)}\zeta^{(123)}) \tag{12}$$

$$\zeta^{(123)} = \frac{\zeta_1\zeta_2^2 + \zeta_2\zeta_3^2 + \zeta_3^2\zeta_1}{\zeta_1\zeta_2 + \zeta_1\zeta_3 + \zeta_2\zeta_3} \tag{13}$$

The mole fractions x_2 and x_3 (and hence x_1) are obtained from the following equations with $i=2, j=3$ or $i=3, j=2$:

$$x_i^{L,V} = \zeta_i + \zeta_i(\zeta_1 + \zeta_i)\left\{\frac{\bar{Q}_i}{\rho^{L,V}} - \frac{\bar{Q}_{i0}}{\rho_c} - \bar{H}_i\right\} - \zeta_i\zeta_j\left\{\frac{\bar{Q}_j}{\rho^{L,V}} - \frac{\bar{Q}_{j0}}{\rho_c} - \bar{H}_j\right\} \quad (14)$$

$$\bar{H}_i = t f^{(123)}(\partial B_c/\partial \zeta_i)_{\zeta_j} \quad (15)$$

$$f^{(123)} = -C_H^{(123)}(1 + C_Z^{(123)}\zeta^{(123)})/B_c \quad (16)$$

where L is liquid and V is vapor. It is straightforward to show the reduction to the binary model when x_1, x_2, or $x_3 = 0$.

To compute the model predictions along a path of constant temperature and overall composition as in Fig. 1, an array of t values is chosen and, starting from the critical point of the charge, a numerical search in ζ_1 and ζ_2 is conducted for the point along the path at the given t. The constraint of constant overall composition is effected, as shown in Fig. 2, by finding the unique pair of liquid and vapor states such that the tie line on a triangle diagram passes through the charge composition point.

4. RESULTS

Our ternary model has been constructed from correlations of the three constituent binaries. Comparisons between the correlations and experiment have been presented for ethane + n-butane [4, 15, 16], n-butane + n-pentane [16], and ethane + n-pentane [5].

We have examined data from Refs. 8 and 9 of 17 different charges at four different temperatures as listed in Table I. Some additional charges were omitted because the overall composition was not reported. Figures 1 and 3 show comparisons between experiment and theory for two of these charges, the first along an ethane-rich, low-temperature path and the second along an n-butane-rich, high-temperature path. The figures show good agreement in both cases, with some deviation on the vapor side at low pressure in Fig. 3. This mixture is interesting in that, as pressure as lowered, n-butane changes from a nonvolatile component (richer in the liquid) to a volatile component (richer in the vapor). The model reproduces the pressure at which the changeover occurs.

For further quantitative analysis, we need a way to compare the experimental and predicted ternary composition. An appropriate comparison is the ratio of the geometric distance between two points on a triangle diagram such as Fig. 2 to the altitude of the triangle, a ratio independent of triangle size:

$$R_x = 2\frac{\sqrt{3}}{3}\left[(x_i^{(1)} - x_i^{(2)})^2 + (x_i^{(1)} - x_i^{(2)})(x_j^{(1)} - x_j^{(2)}) + (x_j^{(1)} - x_j^{(2)})^2\right]^{1/2} \quad (17)$$

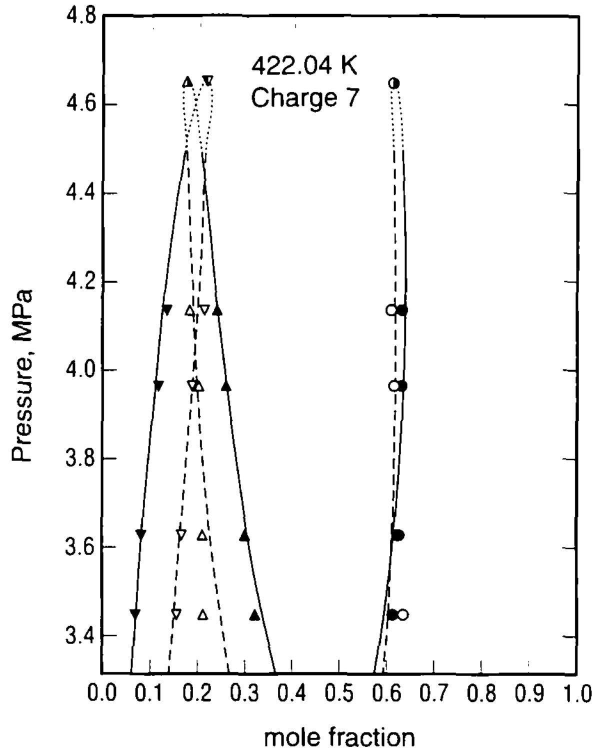

Fig. 3. Critical and coexisting states for charge 7, $T = 422.04$ K. Symbols have same meanings as in Fig. 1.

where $i, j = 1,2$; 1,3; or 2,3; this expression is also invariant under component labeling permutations, as it should be. Table I lists the average comparisons (R_x) for each charge of experiment and model prediction at the same pressure, and only for points within the range of the model; e.g., the lowest points on Fig. 1 are omitted.

As explained in Section 1, the assumption of constant overall composition can be tested with a triangle diagram such as Fig. 2. The tie line joining liquid and vapor points should intersect the point of overall composition, and the perpendicular drop distance from that point to the tie line is a good measure of divergence from constant overall composition. If the respective compositions are x^T for the total, x^L for liquid, and x^V for vapor, then from geometrical considerations, the ratio of drop distance to altitude is

$$R_d = \frac{|x_i^L x_j^V - x_j^L x_i^V + x_i^T x_j^L - x_j^T x_i^L + x_i^V x_j^T - x_j^V x_i^T|}{[(x_i^L - x_i^V)^2 + (x_i^L - x_i^V)(x_j^L - x_j^V) + (x_j^L - x_j^V)^2]^{1/2}} \tag{18}$$

Table I. Deviation Analysis for Ethane + n-Butane + n-Pentane [8, 9]

T (K)	Charge number	$x(C_2)$	$x(C_4)$	ΔT_c (%)	ΔP_c (%)	$\langle R_x \rangle \times 10^2$	$\langle R_d \rangle \times 10^2$
338.71	3	0.840	0.102	0.19	1.43	1.35	0.203
338.71	4	0.830	0.140	0.03	1.28	0.81	0.271
338.71	5	0.880	0.050	−1.63	−2.97	1.78	0.200
338.71	6	0.898	0.022	−2.38	−5.40	1.08	0.244
366.48	1	0.750	0.038	0.24	−2.65	0.82	0.109
366.48	2	0.739	0.070	0.20	−2.44	1.11	0.415
366.48	3	0.723	0.112	0.24	−0.43	1.64	0.919
366.48	5	0.692	0.188	0.41	0.80	1.19	0.256
366.48	6	0.661	0.277	0.25	1.27	1.88	0.992
394.26	1	0.582	0.148	0.02	−2.53	2.27	0.512
394.26	2	0.545	0.235	−0.01	−1.38	1.36	0.459
394.26	3	0.504	0.333	−0.06	1.27	2.04	1.791
394.26	5	0.460	0.438	−0.08	1.60	1.04	0.410
422.04	1	0.430	0.110	−0.03	−3.93	1.93	0.232
422.04	2	0.366	0.240	−0.08	−5.30	2.05	0.063
422.04	3	0.298	0.410	−0.47	−2.76	1.71	0.612
422.04	7	0.215	0.610	−0.65	−0.13	1.34	1.325

where $i, j, k = 1, 2, 3$ and $i \neq j$; like Eq. (17), this expression is invariant under permutations of component labels and triangle size.

Also reported are average discrepancies $\langle R_x \rangle$ between experiment and the model, as well as ΔT_c and ΔP_c, the differences between experimentally stated and model critical properties. An analysis of Table I shows that $\langle R_x \rangle$ is significantly correlated with $\langle R_d \rangle^* + \Delta P_c^*$ and with $\langle R_d \rangle^* + \Delta P_c^* + \Delta T_c^*$, where the asterisk denotes a reduced value obtained from division by the average absolute value over charges of that quantity in Table I. As expected, the phase boundary curves are most accurately described when critical properties are predicted best and when experimental data lie along paths of most nearly constant overall composition.

5. CONCLUSIONS

We have developed a ternary version of the modified Leung–Griffiths model which differs slightly from the earlier work of Lynch et al. [5], and which in general yields a good correlation of the VLE data on ethane + n-butane + n-pentane by Thodos and co-workers [8, 9]. In contrast to the approach of Lynch et al., we have correlated the data under the assumption of constant overall composition.

Lynch et al. also examined the ethane + *n*-butane + *n*-heptane data of Thodos and co-workers [10, 11]. Comparison with experiment for this mixture was less satisfactory, in part because the ethane + *n*-heptane mixture contains such dissimilar fluids that it is somewhat beyond the best range of the modified Leung–Griffiths model for binaries. Consequently, the mixture with *n*-heptane was not considered here.

Our work demonstrates that an accurate correlation of a ternary phase equilibrium surface over an extended critical region can be constructed. The required input is the correlation of the three constituent binary mixtures, and no further parameters are needed. Also, in this example the experimental data can be tested for consistency with the intended thermodynamic path of constant overall composition.

ACKNOWLEDGMENT

This work was supported in part by the Division of Chemical Sciences, Office of Basic Energy Sciences, Office of Energy Research, U. S. Department of Energy.

REFERENCES

1. S. S. Leung and R. B. Griffiths, *Phys. Rev. A* **8**:2670 (1973).
2. M. R. Moldover and J. S. Gallagher, *AIChE J.* **24**:267 (1978).
3. M. R. Moldover and J. C. Rainwater, *J. Chem. Phys.* **88**:7772 (1988).
4. J. C. Rainwater, in *Supercritical Fluid Technology*, J. F. Ely and T. J. Bruno, eds. (CRC Press, Boca Raton, Florida, 1991), p. 57.
5. J. J. Lynch, J. C. Rainwater, L. J. Van Poolen, and D. H. Smith, *J. Chem. Phys.* **96**:2253 (1992).
6. R. T. Jacobsen, W. P. Clarke, S. W. Beyerlein, M. F. Rousseau, L. J. Van Poolen, and J. C. Rainwater, *Int. J. Thermophys.* **11**:179 (1990).
7. D. H. Smith and J. J. Lynch, *Fluid Phase Equilibria* **98**:35 (1994).
8. J. C. Herlihy and G. Thodos, *J. Chem. Eng. Data* **7**:348 (1962).
9. V. S. Mehra and G. Thodos, *J. Chem. Eng. Data* **8**:1 (1963).
10. V. S. Mehra and G. Thodos, *J. Chem. Eng. Data* **11**:365 (1966).
11. V. S. Mehra and G. Thodos, *J. Chem. Eng. Data* **13**:155 (1968).
12. R. B. Grieves and G. Thodos, *I&EC Fund.* **1**:45 (1962).
13. L. J. Van Poolen, *Fluid Phase Equilibria* **58**:133 (1990).
14. J. C. Rainwater and D. G. Friend, *Phys. Lett. A* **191**:431 (1994).
15. L. J. Van Poolen, V. G. Niesen, and J. C. Rainwater, *Fluid Phase Equilibria* **66**:161 (1991).
16. J. C. Rainwater and F. R. Williamson, *Int. J. Thermophys.* **7**:65 (1986).